PERFORMANCE EVALUATION OF WIRELESS NETWORKS

ON CHIP

By

JYUN-LYANG CHANG

A thesis submitted in partial fulfillment of the requirements for the degree of

MASTER OF SCIENCE IN ELECTRICAL ENGINEERING

WASHINGTON STATE UNIVERSITY

School of Electrical Engineering and Computer Science

MAY 2009

To the Faculty of Washington State University:

      The members of the committee appointed to examine the thesis of JYUN-LYANG CHANG find it satisfactory and recommend that it be accepted.

_____

Chair

_____

_____

ACKNOWLEDGEMENT

Performance Evaluation of Wireless Networks on Chip

Abstract

by Jyun-Lyang Chang, M.S.
Washington State University
May 2009

Chair: Partha Pratim Pande

Network on chip (NoC)

The Network-on-Chip (NoC) paradigm has emerged as an enabling methodology to integrate numerous numbers of embedded cores in a single die[1, 2]. The performance gain arising out of adopting NoC is constrained by the performance limitation of the wireline interconnects. With technology scaling, the global wires are quickly becoming the performance obstacle in terms of data communication latency and energy dissipation. Hence, designing the interconnection infrastructure for multi-core chips becomes a major challenge. To alleviate the problems of high latency and energy dissipation in a NoC, different alternative options have been envisioned including wireless NoC, 3D NoC, photonic NoC, and RF-I NoC. In this thesis, we evaluate the performance improvement of the wireless NoCs (WiNoCs) in terms of throughput and latency, and it is compared with the performance of 3D NoCs and traditional 2D wireline NoCs.

TABLE OF CONTENTS

List of Tables

List of Figures

Chapter 1

Introduction

The current trend in System-on-Chip (SoC) design is to integrate numerous numbers of embedded cores in a single die [3]. Designing the interconnection infrastructure for such massive multi-core chips is a major challenge. The Network-on-Chip (NoC) paradigm has emerged as an enabling methodology to design the interconnect architecture for multi-core chips [1, 2]. In spite of all its advantages, traditional NoC employs multi-hop communication, wherein the data transfer between two widely separated blocks gives rise to high latency and energy dissipation. These problems are predicted to become worse with technology scaling. To alleviate the problems of high latency and energy dissipation in a NoC, different alternative options have been envisioned. The conventional two dimensional (2D) integrated circuit (IC) has limited floor-planning choices, and consequently it limits the performance enhancements arising out of NoC architectures. 3D NoC architectures combine the benefits of the two new technologies, viz. 3D ICs and NoCs, to offer unprecedented performance gains in terms of latency, throughput and energy dissipation [4]. Photonic NoCs are predicted to provide ultra-high throughput with minimum latency and lower energy dissipation enabled by advances in nanoscale silicon photonics [5]. Low latency communication in a NoC is also shown to be achieved through RF interconnects, where exchange of data between the embedded cores is guided through on-chip transmission lines [6]. All these emerging

methodologies need further and more extensive investigation to determine their suitability for replacing and/or augmenting existing metal/dielectric-based planar NoC architectures. Due to increased power density on a smaller footprint, heat dissipation is a concern with 3D NoCs. Another problem in 3D NoCs arises from interconnect coupling capacitance and crosstalk. In addition, an electrical coupling between the top metal layer of the first active layer and the device at the bottom of the second active layer needs to be considered. Fabrication complexity of 3D NoCs is another problem. The challenge is to fabricate the subsequent layers, and add them to the chip without damaging the already existing layers. One faulty layer will cause the entire chip to fail, and reduce the overall yield. Photonic NoCs require extensive layout of optical waveguides and on-chip integrated photonic devices, which are non-trivial technological challenges. Also, signal losses in the optical waveguide as well as the signal noise due to coupling between waveguides need further investigation. To sustain high throughput, RF-interconnect based NoCs require multiple very high frequency oscillators and filters. Consequently it is important to explore further alternative strategies to address the limitations of planar metal interconnect-based NoCs. On-chip wireless communication is a step towards this direction. Over the last few years there have been considerable efforts in the design and fabrication of on-chip miniature antennas operating in the range of tens of gigahertz to hundreds of terahertz, opening up the possibility of designing on-chip wireless links [7, 8]. Recent research has uncovered excellent emission and absorption characteristics leading to dipole like radiation behavior in carbon nanotubes

(CNTs), making them promising for use as on-chip antennas for wireless communication.

So far different NoC architectures are proposed, but most of them follow conventional wireline design methods. Below we elaborate characteristics of a few traditional NoC topologies.

- *Mesh*

Mesh is the most widely used NoC topology. It is the most popular architecture due to its short and uniform length of communication links. This architecture consists of an *m x n* mesh of switches interconnecting computational resources (embedded cores) placed along with the switches, as shown in Fig. 1.1 in the particular case of 16 functional embedded cores. Every switch, except those at the edges, is connected to four neighboring switches and one embedded core. In this case, the number of switches is equal to the number of cores in the system. The cores and the switches are connected through communication channels. A channel consists of two unidirectional links between two switches or between a switch and a resource.

Embedded   Wireline NoC   Wireline
Core   Switch   Interconnect
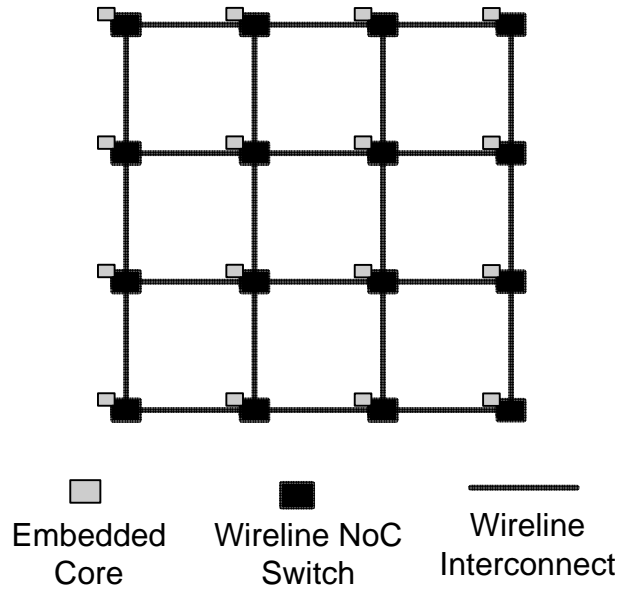
Fig.   1.1: Mesh network

- *BFT*

In a Butterfly Fat Tree (BFT), the embedded cores are placed at the leaves and switches

placed at the vertices. A pair of coordinates is used to label each node, (*l, p*), where *l* denotes

a node's level and *p* denotes its position within that level. In general, at the lowest level, there

are *N* functional cores with addresses ranging from *0* to (*N-1*). The pair (*0, N*) denotes the

locations of cores at that lowest level. Each switch, denoted by *S (l, p)* has four child ports

and two parent ports. The cores are connected to *N/4* switches at the first level. In the jth level

of the tree, there are $N/2^{j+1}$ switches. If we consider a 4-ary tree as shown in Fig 1.2 with four

down links corresponding to child ports and two up links, corresponding to parent ports, then

the total number of switches in level *j=1* is *N/4*. At each subsequent level the number of

required switches reduces by a factor of 2. In this way the total number of switch*es*

approaches $S = N/2$, as *N* grows arbitrarily large [2, 9].
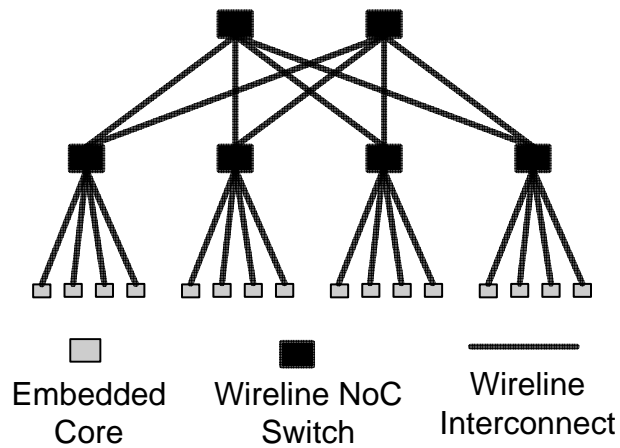
Fig.   1.2: BFT network

As shown in Fig. 1.3, for wireless NoCs (WiNoCs), we propose to divide the network

into multiple small clusters of neighboring cores and called each cluster a subnet. As subnets

are smaller networks, the average path length of intra-subnet communication is shorter than

that of inter-subnet communication. Hence, we propose a hybrid wireline/wireless

architecture where inter-subnet communication is achieved through wireless while

intra-subnet communication is still wireline. For wireless communication, we equip each

subnet with a wireless base station (WB). In each subnet, all cores are connected to the WB

through direct wireline links. When an inter-subnet communication is required, the data is

first sent from the originating core to the WB of the originating subnet and reaches the WB of

the destination subnet through wireless channel. The data then travel from the WB of the

destination subnet to the destination core through direct wireline link. This multiple subnets

architecture with wireless communication makes the WiNoC capable of sustaining high

bandwidth.
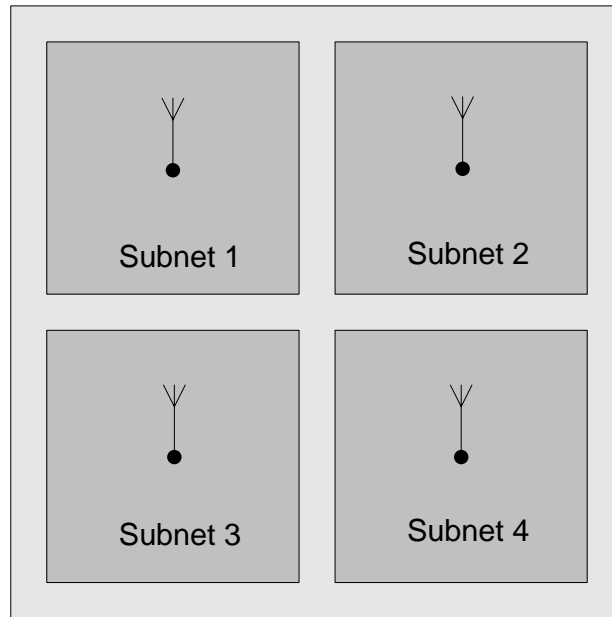
Fig.   1.3: Wireless NoC (WiNoC) architecture

In this work, the performance benefits of the WiNoC are evaluated through cycle

accurate simulations. In this thesis, we will compare and contrast the performance of WiNoC

with other alternatives motioned above, and also with the well known wireline mesh- and

BFT-based NoC architectures, in terms of achievable bandwidth and communication latency.

This thesis is organized in five chapters. Chapter 1 introduces the current trend of the

SoC and the challenges (latency, power) we are facing. Therefore, by introducing the wireless

NoC, we are able to dramatically reduce the latency and the power consumption compare to

the traditional wire line NoC. Chapter 2 covers previous research related to our work. Chapter

3 is an introduction of our cycle accurate simulator. Chapter 4 compares the performance of

wireless NoCs with traditional 2D wire line NoCs and 3D mesh-based NoCs in different

topologies. Chapter 5 concludes our work and gives the directions for the future research.

Chapter 2

Related work

There have been some efforts to provide alternatives to traditional metal interconnect infrastructures for multi-core NoCs through 3D architecture, photonic interconnect and RF interconnect.

According to [10], 3-D architecture allows the performance enhancement due to length reduction of global wires and better connectivity among all cores. Area overhead is also reduced due to significant increase in package density, and power is reduced due to shorter global wires. In [4], it is demonstrated that some 3-D implementation performs better than their 2-D counterparts. A 64-core 3-D mesh is shown in Fig. 2.1.
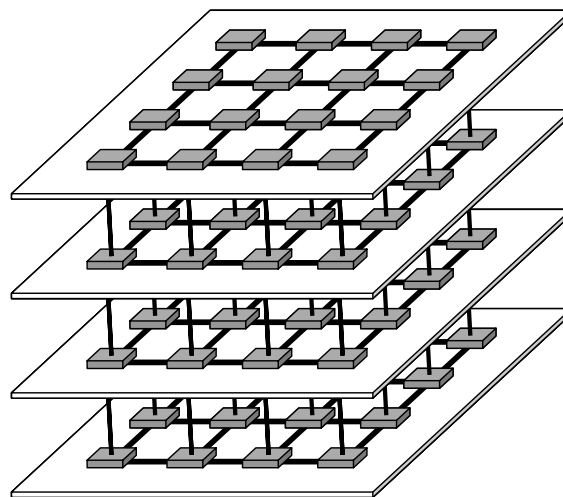
Fig.   2.1: 64-core 3-D mesh architecture

RF interconnect can also be used as an alternative to traditional metal 2D interconnect infrastructure. According to [11], the RF signal is guided through on-chip transmission line and can be used for intra-chip communication to enhance its performance. By using

Frequency Division Multiple Access (FDMA) with multiband frequency synthesizers

together with on-chip transmission lines, RF interconnect channel can be created for data

communication. In [6], design principles for a RF NoC are elaborated. Due to high bandwidth

RF interconnects, the data transmission latency across long distance is reduced. The power

consumption has also been demonstrated to be considerably lower than traditional wireline

2-D NoCs. The proposed RF NoC architecture is shown in Fig. 2.2. The z-shaped RF

transmission line is capable of supporting multiple point to point communications. The

multi-channel communication is achieved through multiple ranges of RF frequency. With

RF/wireline drop points at each corner of the RF transmission line, the hop counts for

communicating between two long distance cores is reduced and hence reduce the

transmission latency.
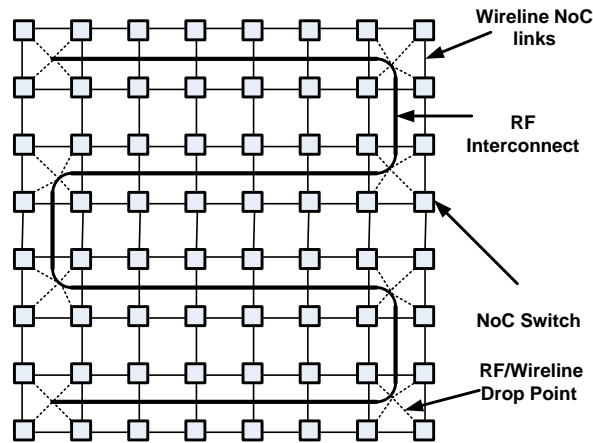
Fig. 2.2: RF interconnect layout

Design principles of a Photonic NoC are elaborated in [5].It is conjectured in [12] that

by using wavelength division multiplexing (WDM) techniques with multiple optical

frequencies to improve data throughput, combined with photonics and optoelectronics,

photonic NoC can be designed. As mentioned in [12], the design of photonic NoCs is based

on the advances made over the past several years in silicon photonics. Fabrication capabilities

involving photonic ICs and integration with commercial CMOS manufacturing open up new

avenues in designing on-chip optical networks. Integration of a fully functional photonic

system on a VLSI die is envisioned. The photonic elements necessary to build a complete

on-chip photonic network, like dense waveguides, switches, optical modulators and detectors,

are now viable for integration on single silicon chip [12]. As an example a recent publication

from IBM [13] demonstrates compact Mach-Zehnder electro-optic modulators, suitable for

sending information between the cores using optical waveguides. The data rate can be as

much as 100 times faster and the communication fabric uses 10 times less power than a

conventional wired system.

The principal advantage of a photonic NoC over an electronic counterpart is its

unprecedented lower power dissipation while sustaining very high bandwidth. In an

electronic NoC the power dissipation arises from the buffer read and write, inter-switch link

traversal and traversing the intra-switch stages. The electronic NoCs are limited by the

achievable bandwidth, which can be a few GHz at most. Consequently to achieve very high

transmission capacity wide links and buffers are needed, which boost the power dissipation.

On the other hand in a photonic NoC the data transfer itself needs negligible power. In optical

data transmission the power dissipation is independent of bandwidth. The only source of

power dissipation is the photonic switch element when it is in the ON state and it is much less

compared to traditional electronic counterparts. Though the electronic control network and the electrical to optical and optical to electrical conversion circuits dissipate more power than the photonic data transfer, still the total power dissipation is much lower than in a wireline NoC. It is estimated in [5] that a photonic NoC with 36 cores at an average bandwidth of 576Gb/s will dissipate around 6 W of power while the corresponding electronic NoC dissipates more than 100 W.

Recently, a wireless NoC based on CMOS Ultra Wideband (UWB) was proposed [14], and a synchronous and distributed medium access control (SD-MAC) protocol was designed for their wireless NoC. It achieves 1 mm transmission range with antennas of length 2.98 mm. Consequently this architecture essentially requires multi-hop communication through wireless channels. The wireless NoC achieves a peak bandwidth of 10Gbps on a single wireless channel for a 16 cores system with 0.18 μm technology node. In [8], the authors demonstrate the performance of silicon integrated on-chip metal zig-zag antennas for intra- and inter-chip communication. The zig-zag antenna is operating in the millimeter wave range of tens of GHz. The antenna size can be decreased if the transmission frequency is increased to THz/optical range. The zig-zag antennas can achieve a communication range of 5 to 10 mm. The above mentioned antennas principally operate in the millimeter wave (tens of GHz) range and consequently their sizes are in the order of few millimeters. If the transmission frequencies can be increased to THz/optical range then the corresponding antenna sizes decrease, occupying much less chip real estate. Characteristics of metal antennas operating in

the optical and near-infrared region of the spectrum of up to 750 THz have been studied [15].

Antenna characteristics of carbon nanotubes (CNTs) in the THz/optical frequency range have

also been investigated [16-18]. Bundles of CNTs are predicted to enhance performance of

antenna modules by up to 40dB in radiation efficiency and provide excellent directional

properties in far-field patterns [19]. Moreover these antennas can achieve a bandwidth of

around 500 GHz, whereas the antennas operating in the millimeter wave range achieve a

bandwidth of 10's of GHz [8]. Thus antennas operating in the THz/optical frequency range

can support much higher data rates. CNTs have several characteristics that make them

suitable as on-chip antenna elements for optical frequencies. With CNT antennas and without

the overlaid waveguide, the on-chip wireless interconnect using optical frequencies can be

build for inter-core communication. In this thesis, we will evaluate the performances for the

alternatives mentioned above, and lay the ground work for developing on-chip wireless

communication.

Chapter 3

Simulator Characteristics

We developed a cycle accurate simulator to explore characteristics of the WiNoC. We assumed wormhole routing [20] as the data transmission mechanism where the data is divided into small fixed length parts called flow control units or flits. The header flit hold the control and routing information. The header flit first establishes a path from source to destination, and data flits follow the path. The important features of the simulator are elaborated below:

3.1 Network construction

In the simulator, we connect embedded cores and switches to form a specific architecture. To establish a connection, we specify the next switch port where the current switch port should be connected to establish the path following the adopted routing algorithm. By doing this for every port in every switch, the network structure is completed. The switches and cores connections for two specific architectures are illustrated in Fig. 3.1.
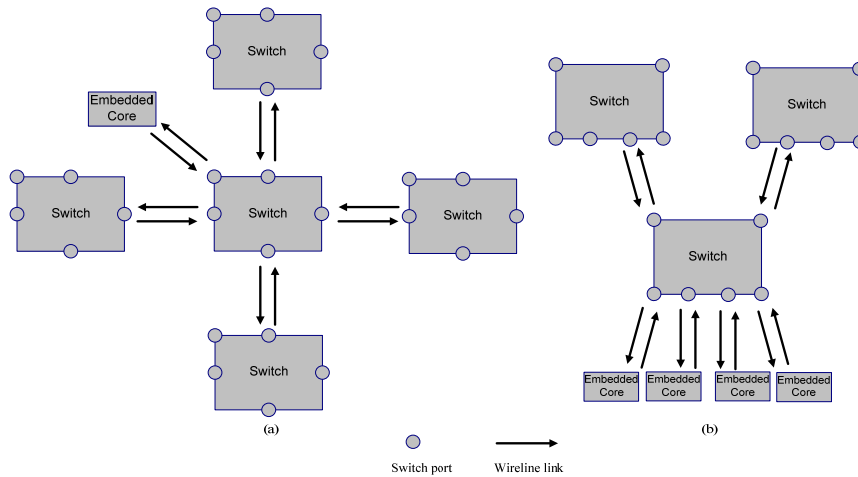
Fig. 3.1: (a) switches for mesh (b) switches for BFT

3.1.1 Switch architecture

As shown in Fig. 3.1, a switch consists of several ports depending on the architecture under consideration. For instance, a switch for mesh architecture has 4 ports connecting to four neighboring switches and 1 port connecting to embedded core while a switch for BFT has 4 ports connecting to embedded cores and 2 ports connecting to the upper level switches. One problem of the switching method is that distinct messages cannot be multiplexed over a physical channel. An entire message has to cross the physical channel before the channel can be utilized by another message. This can greatly degrade the system performance if a flit from a certain packet is blocked in a buffer. Hence, virtual channels are introduced to the switch port, and each switch port may support several virtual channels multiplexed across the port. In WiNoCs, each switch port has 4 virtual channels. Each virtual channel is uniquely indentified by its virtual channel identifier (VCID). Virtual channels of a physical port may be simultaneously filled by incoming flits. Hence, an arbitration mechanism is required at the input port to allow only one virtual channel to access the physical port. The arbitration

mechanism is also required at the output port since flits coming from all input ports may try

to access the same output port simultaneously.

3.1.2 Wireless Base Station (WB)

As introduced in Chapter 1, in the WiNoC the chip is divided into multiple subnets.

Each subnet is equipped with a wireless base station (WB), which is responsible of

establishing wireless communication links between the subnets. As an example, in a 64-core

mesh architecture, the network is divided into 4 subnets, and all 16 cores in each subnet are

connected to its WB through direct wireline link. Whenever data is required to transmit from

one subnet to another, say subnet 1 to subnet 2, the data is first sent from the originating core

to WB of subnet 1 and travels through wireless channel to WB of subnet 2. The data is then

sent from WB to destination through direct wireline link.
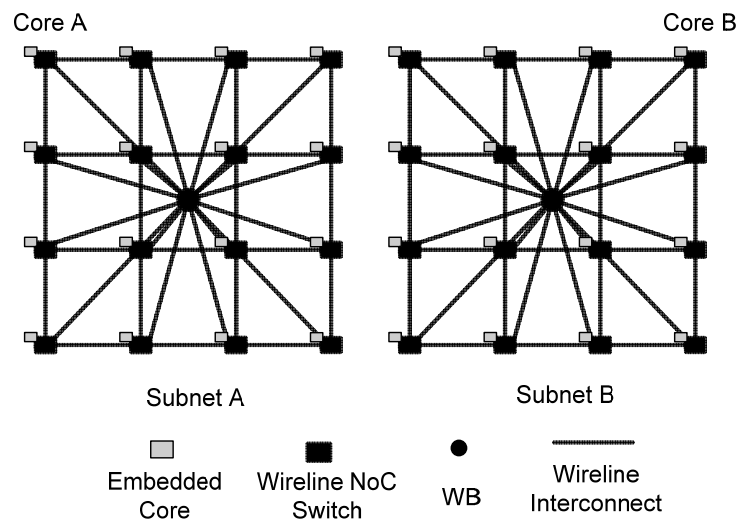
Fig. 3.2: Two mesh_ring subnets with WBs

In Fig. 3.2, if a message is sent from Core A to Core B, it is first routed from Core A to

the WB of Subnet A through direct wireline link, and then travels from WB of Subnet A to

WB of Subnet B through wireless channel; finally, the message is sent to Core B from WB of

Subnet B through direct wireline link.

3.1.3 Network construction (Software perspective)

In this section, we will view the network construction and routing from a software

perspective. The following code is taken from our simulator as an example of how the

network construction and routing is done in the software level.

● Network Construction (Mesh architecture with WB)

```
// ===============================================
for (int a=0;a<numIps;a++){    // injection links
    ports[current_switch_port_index].next = next_switch_port_index;
    ports[next_switch_port_index].next = current_switch_port_index;
}
// =========== Connect all cores to WB ================
for (int i=0; i<(numIps-1); i++){
    ports[current_switch_port_index].next = WB_port_index;
    ports[WB_port_index].next = current_switch_port_index;
}
// ===============================================
```

The above code creates bi-directional connections between all cores in a subnet and their

associate switch, and also between all cores and WB. The statement *ports[X].next = Y*

specifies the current switch port *X* is connected to switch port *Y*. *X* and *Y* are port indexes

within a subnet. For a traditional mesh without WB, the *Connect all cores to WB* section of

the code has to be omitted.

3.2 Traffic Injection

The traffic is first generated by each embedded core and then injected it into its

associated switches. The frequency of generating a flit is determined by the traffic load of the

NoC. If the traffic load is high, the flits will be injected into the system more frequently. The

destinations of the generated flits are determined by the traffic pattern described below.

3.2.1 Uniform Random Traffic:

Traffic is uniformly and randomly distributed among the constituent embedded cores.

Every embedded core can be source or destination with equal probabilities.

3.2.2 Localization

The traffic localization restricts possible destinations of a given source. For

example, with localization factor 0.1, the destination of 10% of the traffic will be

restricted to only the given source's neighboring cores and the destination of the other

90% of the traffic will be randomly distributed among other cores excluding its

neighboring cores.

Below gives an example of software level implementation of localization in mesh

architecture.

```
bool loop=true;
r = float_rand(1);
// ============== Part A ==============
if (r < localization_factor) {
    while (loop){
        loop = false;
        for (int c=0; c < dimensions; c++)
            msgs[i].dest[c]=int_rand(cube_dimensions[c]);
        if (get_cube_address(msgs[i].dest)==get_cube_address(msgs[i].source))
            loop=true;
        if (get_cube_dist_mesh(msgs[i].dest,msgs[i].source)!=1)
            loop=true;
    }
}
// ==================================
// ============== Part B ==============
else {
    while (loop){
        loop = false;
        for (int c=0; c < dimensions; c++)
            msgs[i].dest[c]=int_rand(cube_dimensions[c]);
        if (get_cube_address(msgs[i].dest)==get_cube_address(msgs[i].source))
            loop=true;
        if (get_cube_dist_mesh(msgs[i].dest,msgs[i].source)==1)
            loop=true;
    }
}
        // ==================================
```

The above code is used to generate destinations of the messages injected by each

code. When *r < localization_factor* (Part A), the messages' destinations are localized

around the originating core. Otherwise, when *r >= localization_factor* (Part B), the

messages' destinations will be randomly distributed among the rest of the cores. In

Part A, the loop keeps running until the following conditions

get_cube_address(msgs[i].dest)==get_cube_address(msgs[i].source)   and

get_cube_dist_mesh(msgs[i].dest,msgs[i].source)!=1 are not satisfied. In the first

condition, *get_cube_address(msgs[i].dest)* tells us the destination core of a message

and *get_cube_address(msgs[i].source)* tells us the source core of a message. The first

condition is used to prevent the source and the destination of a message end up in the

same core. The second condition makes sure that the distance between the source core

and the destination core of a message is within one Manhattan distance, which means

the traffic is localized. Similar code is used in Part B, except the second condition is

now used for the purpose to prevent traffic being localized around the source core.

3.2.3 Injection Load

The load factor determines the portion of the traffic, in terms of the maximum

capacity, that is injected into the system. For example, load factor of 1 represents the

maximum capacity. Load factor of 0.1 means we will only be injecting 0.1 of the

maximum traffic into the system.

3.2.4 Injection Type

● Self-Similar Traffic

In the simulator, the self-similar traffic can be generated by aggregating a large number

of ON-OFF message sources. The amount of time each message spends in the ON or the OFF

state is determined by the Pareto distribution, which shows long-range dependence property.

The Pareto distribution is defined as $F(x) = 1 - x^{-\alpha}, 1 < \alpha < 2$. A message stays in the ON state

for $t_{ON} = (1-x)^{\frac{-1}{\alpha_{ON}}}$ and stays in the OFF state for $t_{OFF} = (1-x)^{\frac{-1}{\alpha_{OFF}}}$, where x is an uniformly

distributed random number between 0 and 1, $\alpha_{ON} = 1.9$, and $\alpha_{OFF} = 1.25$ [2].

● Poisson Traffic

The Poisson traffic injection period follows the following exponential PDF

$$f_X(x) = \begin{cases} \lambda e^{-\lambda x} & x \geq 0 \\ 0 & otherwise \end{cases}$$

where λ is the traffic injection rate.

3.3 Traffic Routing & Consumption

There are two parts involved in routing the traffic. The first part is to route the flits

within a switch. According to flits' destination, the algorithm will determine which port the

flit should travel next. The second part is to route the flits among switches. Depending on the

destination, the algorithm will find the next port in another switch and route the flit there.

The header flits play an important role in the simulator. They are used to establish a path

between source and destination and let the data flits travel through that path. The header flits

are routed based on the routing algorithm associated with each architecture. When the header

flit arrives at a switch, it will first be stored in the virtual channels. Then, the simulator will

look through every virtual channel of every port within that switch to find the stored header

flit and retrieve the destination information. According to the destination information, the

next port within the switch will be assign to the header flit. When the header flits encounter

collisions, which means two or more headers at the same switch intend to go to the same

destination port within the switch, a select function will be called to deal with the problem.

The methods that we use to determine which header flit has the priority to route through a

switch in a collision situation are *port orders, oldest first,* and *highest priority. Port orders*

means the header flits will route through the switch base on the order of the ports it's at.

Oldest first means the header flits which have been held at the switch for the longest time

have the priority to go through. *Highest priority* means the header flits will route through the

switch based on the priority information stored in them. Once the header flit establishes a

path, the data flits follow it to the destination. The cores are constantly monitoring arrival of

header flits. If a core detects a header flit, it knows the following (N-1) flits will be the data

flits (N = 64). Therefore, it initializes a data consumption countdown and counting from 0 to

(N-2) to finish the consumption of one message.

3.4 Conclusion

In this chapter we elaborated the characteristics of the simulator used to explore the

performance trade-offs for the WiNoCs. We explained how the simulator is used to model

different components of the WiNoC. Beginning by introducing the network construction and

the switch architecture followed by the characteristics of the injection traffic, finally, the

routing mechanism and flit consumption process are explained. In the next chapter, we will

use the simulator to evaluate the performance of WiNoCs and traditional NoCs.

Chapter 4

Performance evaluation

In this chapter, our aim is to evaluate performance of the WiNoCs compared to the conventional 2D wireline and 3D mesh-based NoC architectures. Here we are principally concerned with the network-level characteristics. Consequently the performance metrics considered in this evaluation are the network throughput and latency. These two parameters are defined below:

4.1 Performance Metrics

- *Latency:* Latency is defined as the time period between the injection of a message's header flit and the reception of the same message's tail flit at the destination core. In the simulator described in chapter 3, the latency is obtained in units of clock cycles.

- *Throughput:* Throughput is a metric that quantifies the rate at which message traffic can be sent across a communication fabric. It is defined as the average number of flits arriving per embedded core per clock cycle, so the maximum throughput of a system is directly related to the peak data rate that a system can sustain. Accordingly, it is important to note that a throughput of 1 corresponds to every node accepting one flit in every clock cycle.

4.2 Experimental setup

Simulator parameters	
Number of embedded cores	64
Buffer Depth (flits)	2
Virtual Channels	4
Message Length (flits)	64
Flit size	32 bits

Table 4.1: Simulator parameters

To carry out the evaluation process we considered a system with 64 embedded cores

and mapped them to different architectures under consideration. The experimental parameters

are shown in Table 4.1. Each switch port has 4 virtual channels and each of them can store up

to 2 flits. A single message consists of 64 flits and each flit is of size 32bits.

As mentioned in Chapter 1, for the wireless NoC, the whole network is divided into 4

subnets and each subnet consists of 16 cores. Intra-subnet communications are all based on

traditional wireline links while inter-subnet communications are done through wireless

channels. All the subnets have a wireless base station (WB), which is responsible for

establishing the wireless channels among the subnets. Two subnet architectures of WiNoC are

considered: mesh and hybrid ring-star.

● *Mesh*

In this topology the cores in a subnet are interconnected among themselves by a

wireline mesh network. This mesh subnet has NoC switches and links as in a standard mesh

based NoC. Packet routing within the subnet follows dimension order (e-cube) routing. In

addition to this underlying mesh all the individual switches have direct wireline links to a WB as shown in Fig. 4.1 (a).

- *Hybrid Ring-Star*

In this subnet topology all the cores are connected on a ring to two nearest neighbors on either side through conventional wireline NoC switches. In addition there is a central switch which is attached to all the cores as well as the WB as shown in Fig. 4.1 (b). The central switch provides additional connectivity compared to a simple ring structure. Data routing follows a simple algorithm wherein, if the destination core is within two hops on the ring from the source then the data is routed along the ring. If the destination core is more than two hops away then the data routing takes place via the central switch. Thus within the subnet each core is at a distance of at most two hops from any other core. The central switch is connected to the WB and all inter-subnet packets are routed to the WB from the central switch.

The performance of the two above mentioned WiNoCs are compared with traditional 2D wireline mesh, wireline BFT, and wireline hierarchical mesh. In the hierarchical mesh, the whole network is divided into 4 subnets. All the switches in each subnet connect to 4 of their neighboring switches and connect to two additional switches in two other subnets as shown in Fig. 4.1 (c). For clarity not all connections are shown in Fig. 4.1 (c). The extra connectivity of each switch reduces the hop count between source and destination. This factor contributes to the improved throughput and latency characteristic compare to a traditional wireline mesh.
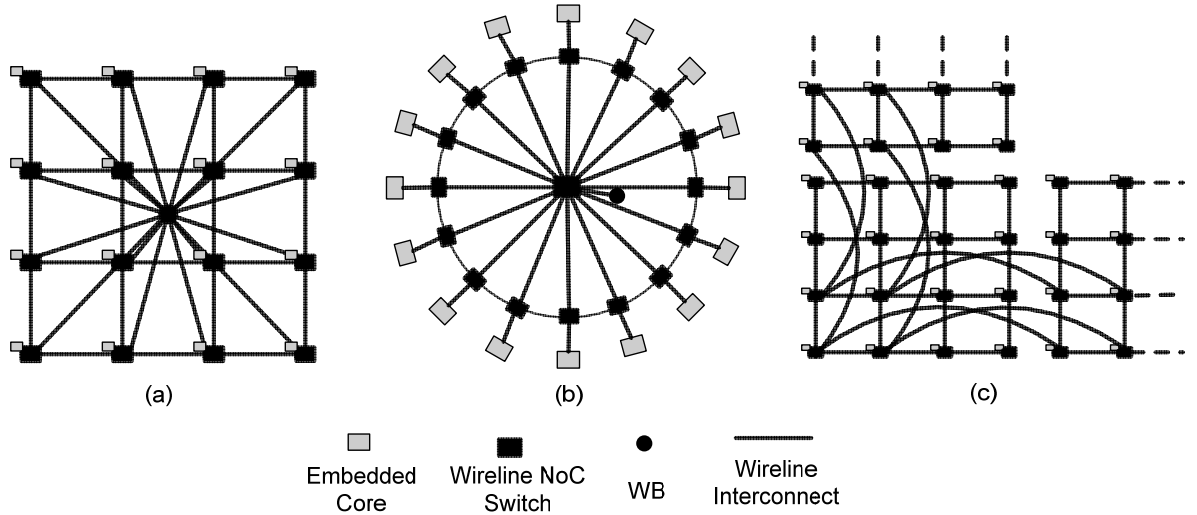
Fig. **4.1: (a) WiNoC MESH** **(b)WiNoC hybrid RING-STAR** **(c) Wireline HI-MESH**

● *3D Mesh & Stacked Mesh*

The performance of the two WiNoCs architectures is also compared with 3D NoC architectures. Two 3D NoC architectures, viz. the 3D mesh and stacked mesh are considered for the performance evaluation. Below we briefly elaborate the characteristics of these two 3D architectures.

■ *3D Mesh*

A 64-core 3D mesh architecture is shown in Fig. 4.2 (a). All 64 cores are mapped onto four layers; each layer consists of 16 cores. As shown in Fig. 4.3 (a), 3D NoC employs 7-port switches: one port to the embedded core, two ports to the upper and lower layers, and four ports to four adjacent switches within the layer. Due to smaller networks of each layer and extremely short interconnects between layers, the 3D mesh architecture presents a significant performance improvement compares to the traditional

25

2D wireline mesh.

(a)   (b)

Embedded cores   Interconnect   Bus
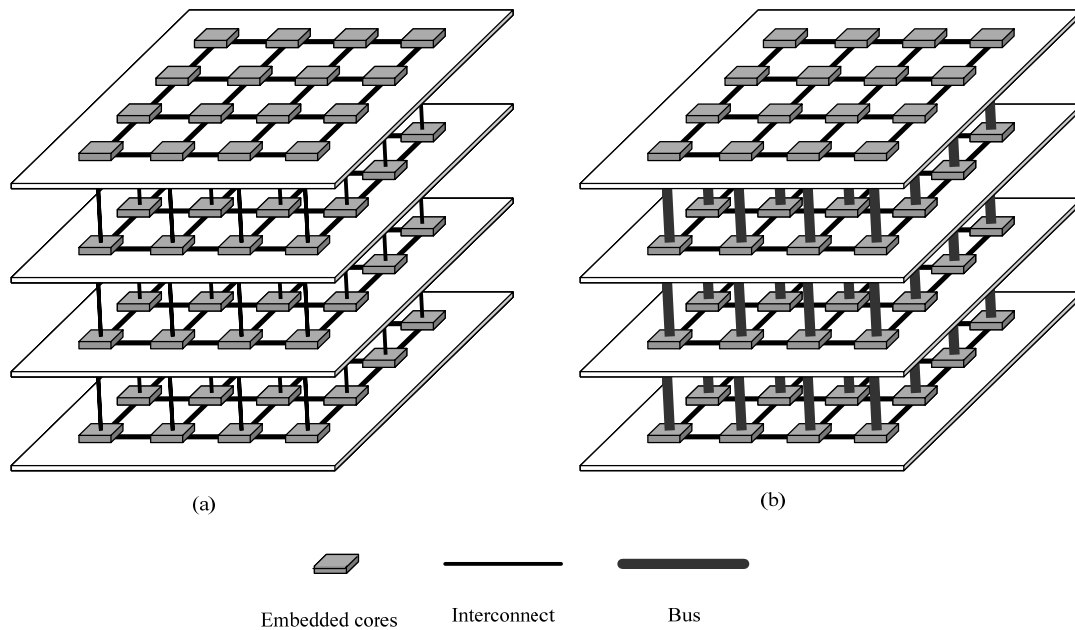
Fig.   4.2: (a) 3D Mesh (b) Stacked Mesh

■   *Stacked Mesh*

Fig. 4.2 (b) shows a stacked mesh architecture. It takes the advantage of extremely

short inter-layer distances and utilizes buses for inter-layer communication. Since the

distances between each individual layers are small, the lengths of the buses spanning the

entire four layers are also small. This makes the bus a suitable interconnection scheme

for the stacked in the z-dimension. In addition, each bus only has four nodes; each of

them connects to an individual layer. The small number of nodes contributes minimum

capacitances to the bus, which maintains the high performance of z-dimension

communication. As shown in Fig. 4.3 (b), stacked mesh employs 6-ports switches: one

to the embedded core, one to the bus, and four to the adjacent four switches within the

layer.
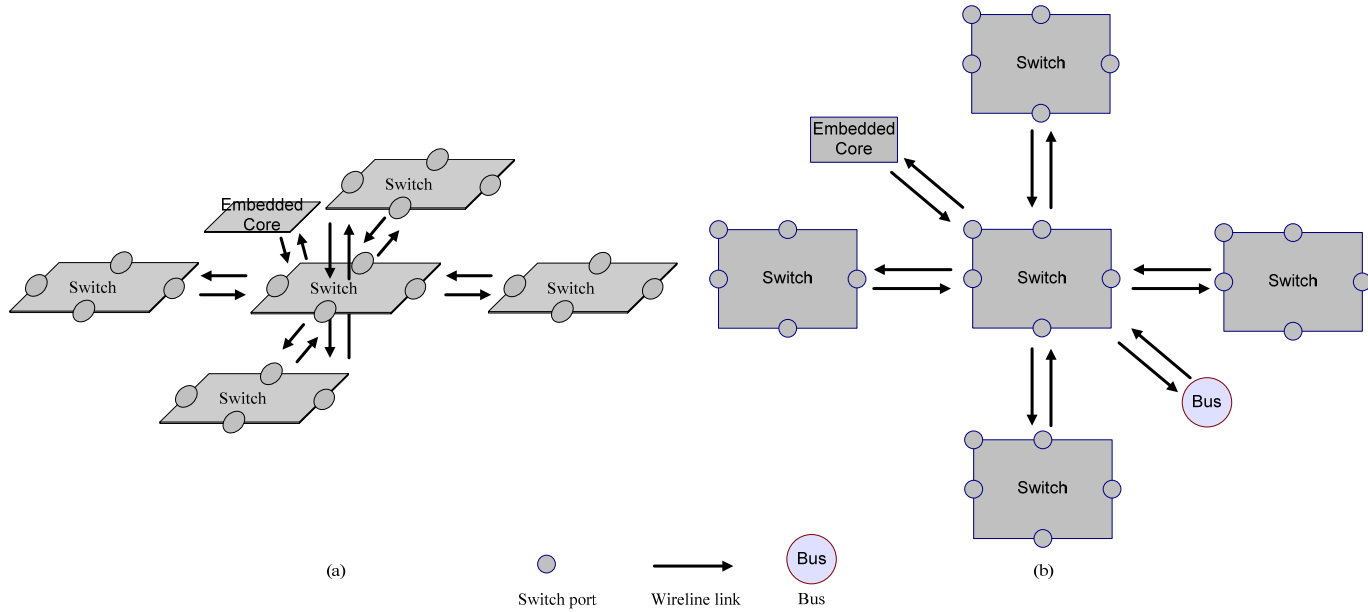
Fig. 4.3: Switche architectures of (a) 3D Mesh, (b) Stacked Mesh

4.3 Experimental Results: Throughput & Latency

To evaluate the performance of WiNoCs, traditional 2D wireline NoCs, and 3D

mesh-based NoCs, we consider the throughput and latency characteristics of 64 cores base

NoCs. Here, we evaluate two WiNoC architectures (hybrid ring-star, mesh), three completely

wireline architectures (mesh, BFT, and hierarchical mesh), and two 3D mesh-based

architectures (3D mesh, stacked mesh).

4.3.1 Throughput vs. Injection Load

The following two figures show the throughput characteristics of different NoC

architectures with respect to injection load. Injection load is defined by the number of flits

injected by each core per cycle. Fig. 4.4 shows the comparison between WiNoC architectures

and wireline 2D architectures.
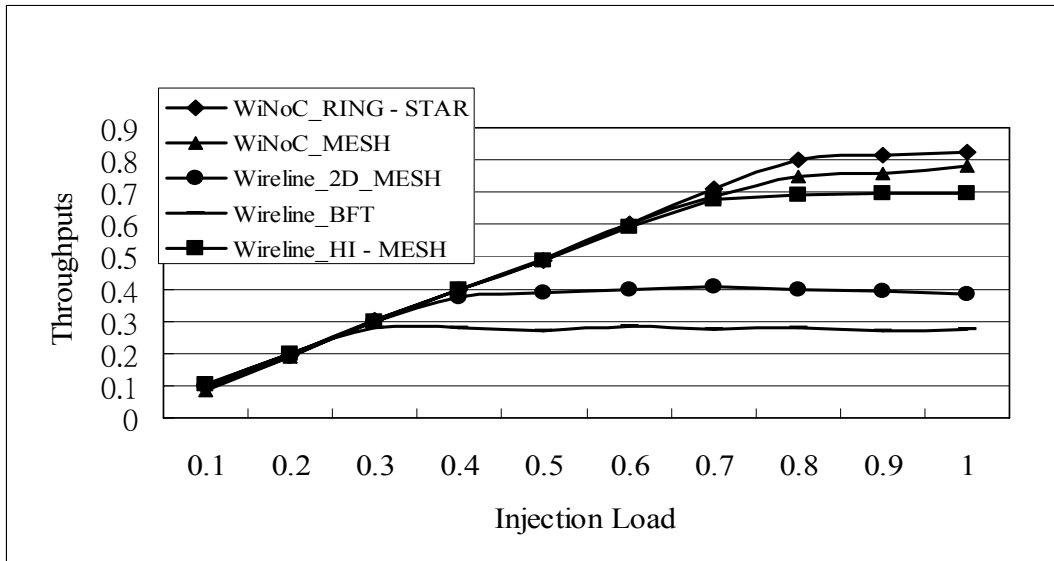
Fig.   4.4: Throughput vs. Injection Load (comparison with 2D NoCs)
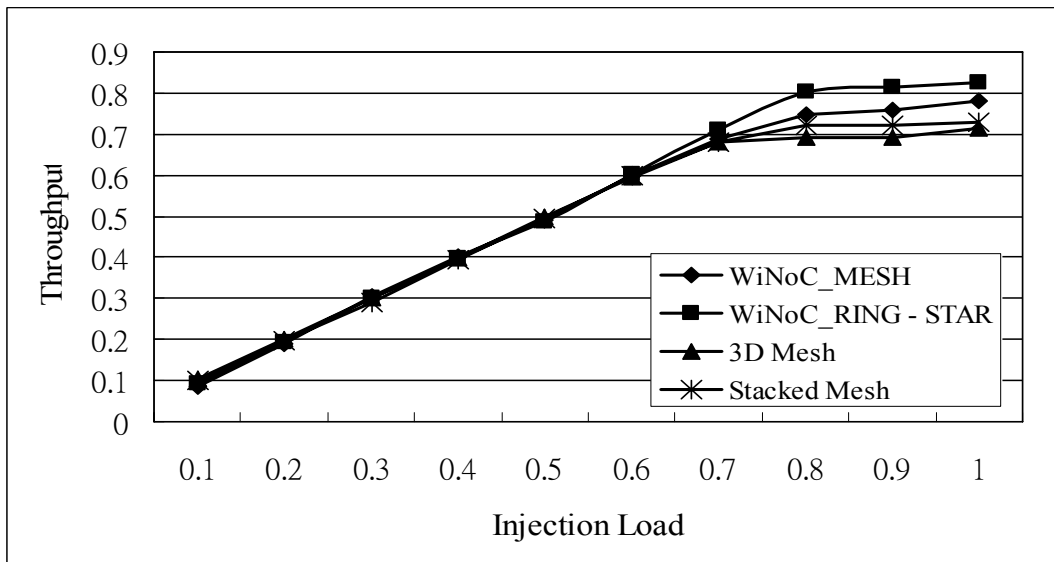
Fig.   4.5: Throughput vs. Injection Load (comparison with 3D NoCs)

Fig. 4.4 clearly shows the throughput advantage of WiNoC compare to traditional 2D

wireline architectures. This is due to the fact that wireless links between the subnets

affectively reduce the hop count while communicating between two long distance cores. In

other words, the flits in WiNoC need to travel less stage between a pair of source and

destination than traditional 2D wireline architectures. Since average hop count of wireline

BFT and wireline mesh is higher due to multi-hop communication, we see wireline BFT and

mesh performance worse in this category. On the other hand, hierarchical mesh is the only completely 2D wireline architecture which has similar throughput characteristic as that of WiNoC. It is due to the increased connectivity of hierarchical mesh, which effectively reduce the hop count between two far away cores.

Fig. 4.5 depicts the comparative evaluation between the WiNoC architectures and 3D mesh-based architectures. It shows the throughput advantage of WiNoC compared to the 3D mesh-based architectures. However, the 3D architecture is able to closely match the throughput performance of WiNoCs due to its high efficiency z-dimension communication, which reduces the hop counts when communicating between two far away cores. As shown in [21], the authors determined the average hop count of the 64-core 3D mesh to be 3.51, which has a 40% reduction compare to 5.33 average hop count of the 64-core 2D wireline mesh. As a result, we can expect a corresponding increase in throughput of the 3D mesh, which shows in Fig. 4.5. Also notice that stacked mesh performs slightly better than 3D mesh. It is because the z-dimension bus of the stacked mesh reduces the hop counts of inter-layer communication slightly compare to those of 3D mesh. Between 2 WiNoC architectures, the hybrid ring-star architecture performs better than the mesh architecture. It is due to the higher connectivity of hybrid ring-star architecture, which means the average hop count of hybrid ring-star is lower. Also notice that as we increase the injection load, wireline BFT and wireline MESH saturate very quickly resulting in low throughput. On the other hand, 2 WiNoC architectures, wireline hierarchical mesh, and 3D architectures can handle way more traffic.

■ Maximum bandwidth

The bandwidth is obtained as the number of bits per second successfully

transmitted to their destinations based on a 3GHz clock. The maximum sustainable

bandwidths for WiNoC ring-star and WiNoC mesh architecture are 54Tbps and 49Tbps

respectively. We can see in Table 4.2, the two WiNoC architectures can sustain

considerably more bandwidth than 2D wireline mesh and wireline BFT. Although the

sustainable bandwidths of 3D architectures come very close to those of WiNoCs due to

very efficient z-dimension links of the 3D architectures, the performance of WiNoC

architectures is still the best in this category.

	Maximum Bandwidth (Tbps)
WiNoC_RING-STAR	54
WiNoC_MESH	49
Wireline_MESH	25
Wireline_BFT	17
Wireline_HI-MESH	44
3D Mesh	44
Stacked Mesh	45

Table 4.2: Maximum bandwidth

4.3.2 Latency vs. Injection Load
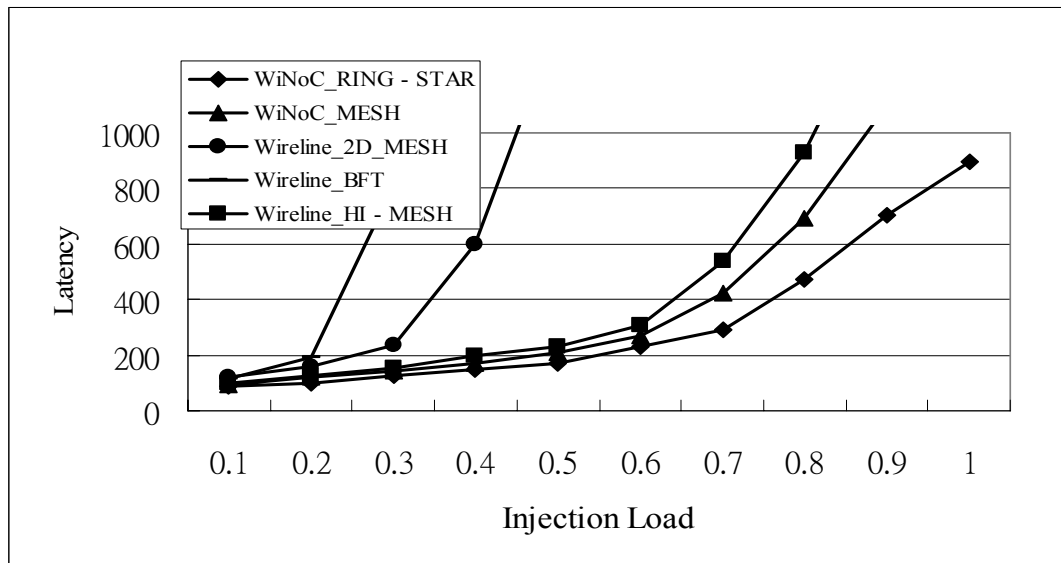
Fig.   4.6: Latency vs. Injection Load (comparison with 2D NoCs)
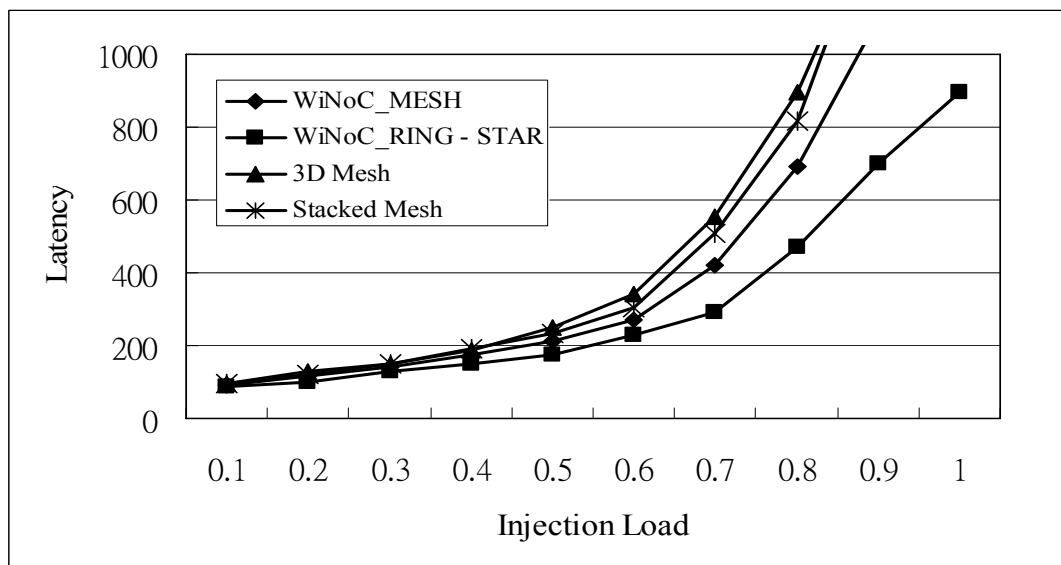
Fig.   4.7: Latency vs. Injection Load (comparison with 3D NoCs)

The latency characteristic of the network is closely related to the throughput

characteristic. When the throughput of a network increases, the latency of it decreases. As

shown in Fig. 4.6 and Fig. 4.7, the 2 WiNoC architectures have the lowest latency among all

architectures. This shows the same performance advantages of WiNoCs as seen in the

previous section.

4.3.3 Throughput vs. Traffic Localization

For the previous analysis, we assumed that the traffic is random and uniformly distributed among all the embedded cores. However, in a NoC, different functions are mapped to different parts of the chip. Hence, the traffic is expected to be localized to different degrees. We therefore study the effects of traffic localization on performance of WiNoCs, traditional 2D wireline NoCs, and 3D mesh-based architectures.

In BFT, the localized traffic is constrained to within the cluster of each sub-tree. In WiNoC mesh, 2D wireline mesh, and 3D mesh, the localized traffic is constrained to within the destination located at the shortest Manhattan distance. In WiNoC ring-star, the destination of the localized traffic is limited to two adjacent cores of its originated core.

In stacked mesh architecture, Li et al.[22] suggested much of the traffic should occur in z-dimension to take advantage of high efficiency buses. As a result, processor and memories are often place along the z-dimension because a large portion of the traffic occurs between them. In this case, the traffic will be highly localized. Therefore, we consider the localized traffic for stacked mesh to be constrained within the z-dimension buses.

The following two figures show the throughput characteristics of different NoC architectures with respect to traffic localization. Fig. 4.8 compares the performance between WiNoC architectures and wireline 2D architectures. Fig. 4.9 compares the performance between WiNoC architectures and 3D mesh-based architectures.
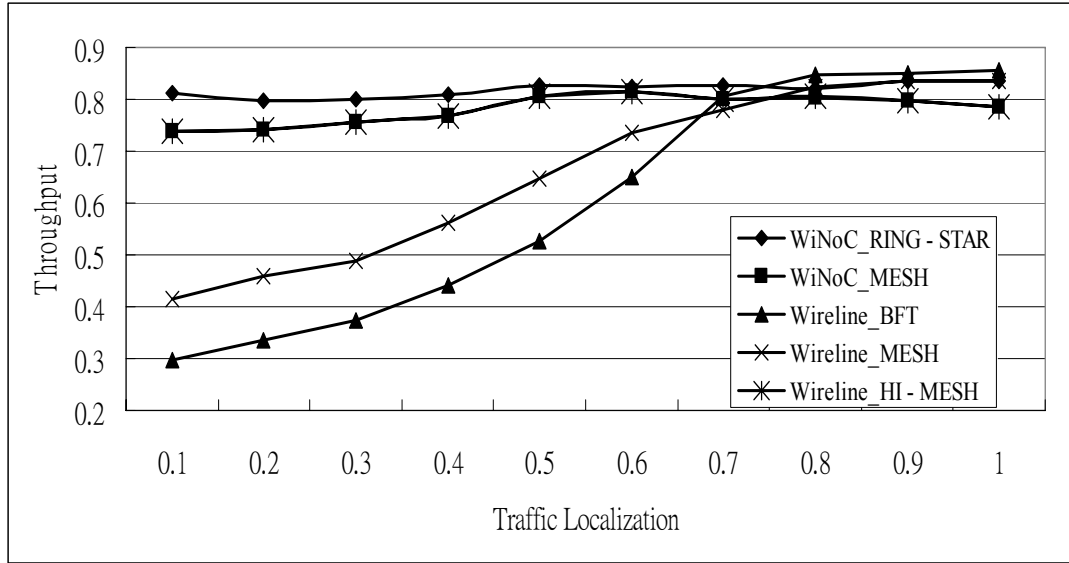
Fig. 4.8: Throughput vs. Traffic Localization (comparison with 2D NoCs)
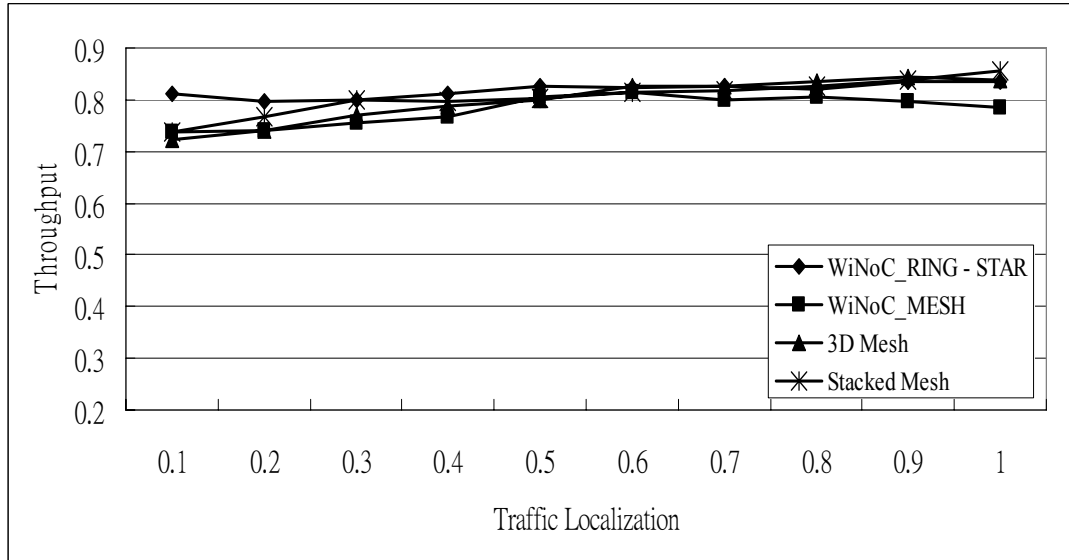
Fig. 4.9: Throughput vs. Traffic Localization (comparison with 3D NoCs)

Fig. 4.8 depicts the effects of traffic localization on throughput. The 2 WiNoCs still

possess performance advantage among the best in this category. As seen in Fig. 4.8, the

throughputs of wireline BFT and wireline mesh improve significantly while localized traffic

is applied. For wireline BFT, because of the highly localized traffic within each sub-tree, the

average hop counts between source and destination reduce considerably. The average hop

counts of wireline mesh also reduces as the traffic localization increases resulting in

performance boost. However, in order to achieve comparable bandwidth with the WiNoCs

and 3D NoCs, we have to have at least 70% of localized traffic.

Notice that the throughput characteristic of the two WiNoC architectures does not

improve much by traffic localization. Their throughput only increase slightly with higher

localization factor. This is because of the average hop counts of the WiNoC architectures are

already low, they can not reduce much more due to localized traffic. With traffic localization,

the maximum sustainable bandwidth of WiNoC hybrid ring-star becomes 55Tbps which only

has 1.8% gain compares to 54Tbps maximum bandwidth of the non-localized hybrid ring-star.

For WiNoC mesh, the maximum bandwidth becomes 53Tbps which has 8.2% gain compares

to 49Tbps maximum bandwidth of the non-localized mesh. We can see that WiNoC mesh

benefits more from localized traffic.

With traffic localization, the bandwidths of 3D mesh and stacked mesh increase to

52Tbps and 51Tbps respectively. As seen in Fig. 4.9, 3D architectures have very similar

throughput characteristics as those of WiNoCs. The performance of the 3D architectures also

does not improve much with localized traffic. It is because the already low averages hop

counts that do not scale very well with localized traffic.

4.3.4 Latency vs. Traffic Localization

Fig.   4.10: Latency vs. Traffic Localization (comparison with 2D NoCs)

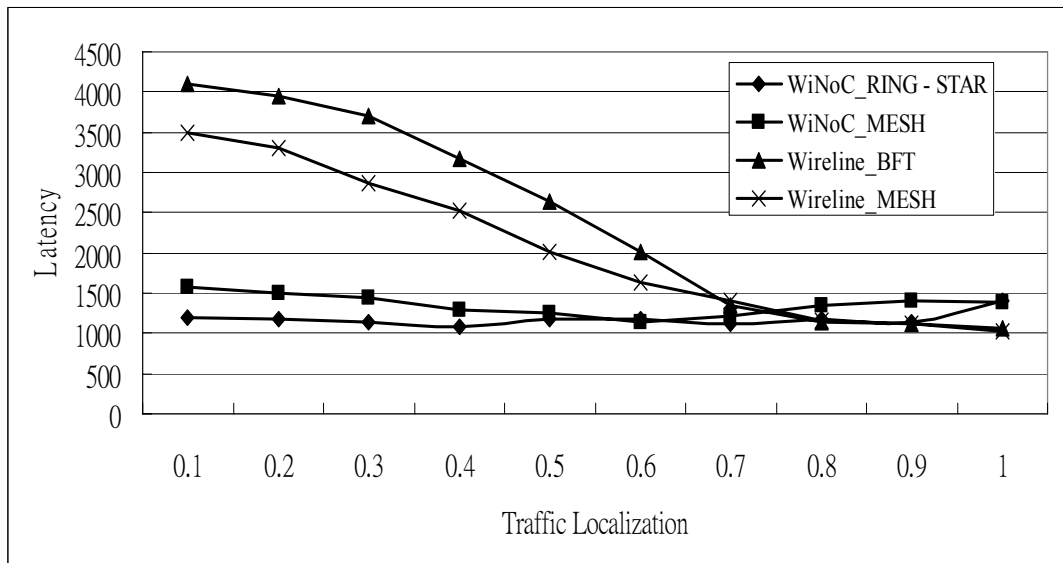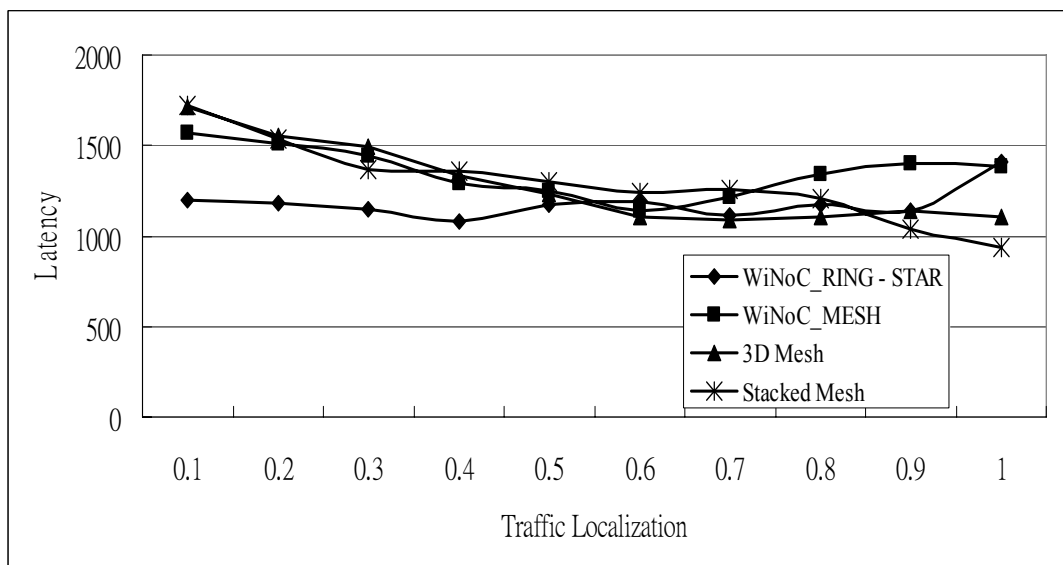**Fig.   4.11: Latency vs. Traffic Localization (comparison with 3D NoCs)**

Fig. 4.10, demonstrates that the 2 WiNoC architectures have great latency characteristics.

We see that, in Fig. 4.10 and Fig. 4.11, the latency performances of all the architectures are

very similar except for wireline BFT and wireline mesh. This agrees with the observations we

got in the previous section.

4.4 Conclusion

In this chapter, we have evaluated throughput and latency characteristics of two WiNoC architectures (hybrid ring-star, mesh) with respect to three conventional 2D wireline architectures (mesh, BFT, HI-mesh) and 3D mesh-based architectures (3D mesh, stacked mesh). The simulation results show the WiNoC architectures have much better performance than traditional 2D wireline mesh and wireline BFT. This is due to the fact that wireless links between the subnets affectively reduce the hop count while communicating between two long distance cores. The performance of the wireline HI-mesh architecture is close to those of WiNoCs due to the increased connectivity of hierarchical mesh, which reduces the hop count between two far away cores. Also, 3D architectures present similar performance as that of WiNoCs. It is because when communicating between 2 long distance cores, the high efficiency z-dimension links affectively reduce the hop counts between the 2 cores, and therefore improves the performance of the 3D architecture

Chapter 5

Conclusions and Future work

5.1 Conclusions

The current trend in System-on-Chip (SoC) design is to integrate numerous numbers of

embedded cores in a single die. The biggest challenge in the design of such massive

multicore chips is their interconnection infrastructure. The Network-on-Chip (NoC) paradigm

has emerged as an enabling methodology to design the interconnect architecture for

multi-core chips. In spite of all its advantages, traditional wire-based NoC employs multi-hop

communication, wherein the data transfer between two long distance cores gives rise to high

latency and energy dissipation. These problems can be resolved if the long distance multi-hop

communication links in a NoC are replaced with single-hop high-bandwidth wireless links.

In this thesis, we have demonstrated the performance advantages of two WiNoC

architectures (hybrid ring-star, mesh) in terms of network-centric parameters, like throughput

and latency by comparing them with traditional 2D wireline NoCs (BFT, mesh, Hi-mesh) and

3D mesh-based architectures (3D mesh, stacked mesh). We developed a versatile simulator,

which can be used to obtain the performance of the wireless NoCs (WiNoCs) under various

realistic traffic conditions. This simulator can accept various network architectures and traffic

patterns (both spatial and temporal) as inputs and it predicts the performance of the WiNoCs.

This kind of simulator helps the designer to quickly obtain a rough estimate of the expected

performance and the resources used for any WiNoC architectures. With the help of this

simulator we have evaluated all the above architectures in terms of their throughput and

latency characteristics while varying traffic injection load and traffic localization factor. In

chapter 4 we have shown that, without any kind of traffic localization, the maximum

bandwidth of WiNoC ring-star and WiNoC mesh are 54 Tbps and 49 Tbps respectively. This

performance is much higher than the traditional 2D wireline mesh and BFT architectures,

which is only 25 Tbps and 17 Tbps respectively. In order for the 2D wireline mesh and BFT

architectures to match the performance of WiNoCs, at least 70% localized traffic has to be

employed. 3D mesh-based architectures, on the other hand, have much better performances

than the conventional 2D mesh and BFT. 3D mesh and stacked mesh architectures achieve

maximum bandwidths of 44 Tbps and 45 Tbps respectively. With localized traffic, the 3D

mesh-based architectures can almost match the performances of WiNoCs.

5.2 Future Work

The research performed for this thesis has several far reaching directions as discussed below:

5.2.1 Optimization of network configuration

In this thesis, the network of WiNoC is divided into four equal quadrants; each one is

defined as a subnet. Under a given network size, there are various ways of arranging the

subnets as well as the subnet size. The optimal way of setting up the subnets is yet to be

studied.

5.2.2 Comparison among all alternatives

In addition to WiNoCs and 3D architectures, investigations regarding photonic NoCs [5, 12] and RF-interconnect NoCs [6, 11] have been done as potential alternatives to traditional 2D wireline architectures. Although the research of photonic NoC shows a promising sustainable bandwidth, problems such as fabrication difficulty of the on chip wave guides and optical switch mechanism still need further investigation. Also, it is a challenge for RF-interconnect based NoCs to place multiple very high frequency oscillators and filters on chip. Given that each alternative has its own advantages and shortcomings, a comprehensive comparison among all these alternatives needs to be performed.

For a comprehensive comparison, throughput and latency are not the only concerns. Though latency and throughput characterize a network, but for an on-chip network the following parameters are important factors and they need to be considered for a complete and exhaustive performance evaluation.

● Power Dissipation

In traditional wireline NoCs, the interconnect infrastructure dissipates a large percentage of power. This is shown to approach 50% in some applications [23]. Therefore, the power dissipation is a key factor for all the emerging alternative NoC architectures. Though the 3D, Photonic and RF-interconnect based NoCs are shown to be more power efficient than traditional planar NoCs, but how they will perform compared to a WiNoC is a very important concern. Success of WiNoC paradigm will depend on how it performs with respect to this

parameter.

- Fabrication Difficulty

The success of all these emerging technologies will depend on their manufacturability. So far both 3D and Photonic NoCs suffer from manufacturability issues. One serious factor influencing the transition towards 3-D integrations is die yield, which in the case of 3-D circuits depends on factors like pattern mismatch between different layers and vertical via failure. An additional difficulty is to be able to fabricate the subsequent layers or add them to the IC without damaging the already-existing layers. For instance, high-temperature processes such as thermal growth and diffusion can severely affect the previous layers. Also, one faulty layer can cause the whole 3D assembly to fail, reducing the overall yield. Consequently increasing the number of active layers affects the yield of a 3D chip. Similarly though there is tremendous progress in silicon photonics for the last few years, but still the technology to integrate all the necessary components of a Photonic NoC in a single die is far from mature. Comparatively the RF-interconnect based NoC can be designed using existing CMOS technologies. In case of WiNoC if we depend on on-chip RF antennas then also there are no big manufacturability issues. But if the advantages of emerging carbon nanotube antennas need to be exploited to design the WiNoC then that will again involve different manufacturing issues. All these factors need to be incorporated for a complete performance evaluation

- Area Overhead

The silicon area overhead for all these emerging NoCs need to be considered. Area overhead

arising from the NoC switches, integration of various components, like antennas, photonic

components etc. need further examination.

- Heat Dissipation

Heat dissipation is a key factor that affects the stability of a chip. This is a potential problem

for 3D NoCs. Due to 3D structure, the size of each layer in 3D NoC is reduced. It results in a

sharp increase in power density. As mention previously, the interconnect infrastructure

dissipates a large percentage of power. Therefore, the major heat dissipation of 3D NoC

comes from the interconnection network. While evaluating performance of WiNoC with 3D

NoCs heat dissipation needs to be accounted for.

5.3 Summary

NoC has emerged as an enabling methodology for integration of huge number of

embedded cores on a single die. The interconnect infrastructure is known as the performance

bottleneck of traditional 2D wireline NoCs. In this thesis, we have proposed an alternative

architecture (WiNoC) to resolve this problem. We have demonstrated that the performance of

the WiNoCs has significant improvement compare to the traditional 2D wireline NoCs. We

also compared the performance of the WiNoCs to the 3D mesh-based NoCs, which is known

to have a significant performance gain over the traditional 2D wireline architecture. WiNoCs

still possess its performance advantages against 3D mesh-based architectures.

BIBLIOGRAPHY

[1]   L. Benini and G. De Micheli, "Networks on chips: A new SoC paradigm," *Computer,* vol. 35, pp. 70-+, Jan 2002.

[2]   P. P. Pande, C. Grecu, M. Jones, A. Ivanov, and R. Saleh, "Performance evaluation and design trade-offs for network-on-chip interconnect architectures," *Ieee Transactions on Computers,* vol. 54, pp. 1025-1040, Aug 2005.

[3]   S. R. Vangal, J. Howard, G. Ruhl, S. Dighe, H. Wilson, J. Tschanz, D. Finan, A. Singh, T. Jacob, S. Jain, V. Erraguntla, C. Roberts, Y. Hoskote, N. Borkar, and S. Borkar, "An 80-tile sub-100-W TeraFLOPS processor in 65-nm CMOS," *Ieee Journal of Solid-State Circuits,* vol. 43, pp. 29-41, Jan 2008.

[4]   V. F. Pavlidis and E. G. Friedman, "3-D topologies for networks-on-chip," *Ieee Transactions on Very Large Scale Integration (Vlsi) Systems,* vol. 15, pp. 1081-1090, Oct 2007.

[5]   A. Shacham, K. Bergman, and L. P. Carloni, "Photonic networks-on-chip for future generations of chip multiprocessors," *Ieee Transactions on Computers,* vol. 57, pp. 1246-1260, Sep 2008.

[6]   M. F. Chang et al, "CMP Network-on-Chip Overlaid With Multi-Band RF-Interconnect," *Proceedings of IEEE International Symposium on High-Performance Computer Architecture (HPCA),* pp. 191-202, 16-20 February 2008.

[7]   K. Kempa, J. Rybczynski, Z. P. Huang, K. Gregorczyk, A. Vidan, B. Kimball, J. Carlson, G. Benham, Y. Wang, A. Herczynski, and Z. F. Ren, "Carbon nanotubes as optical antennae," *Advanced Materials,* vol. 19, pp. 421-+, Feb 5 2007.

[8]   J. J. Lin, H. T. Wu, Y. Su, L. Gao, A. Sugavanam, J. E. Brewer, and K. O. Kenneth, "Communication using antennas fabricated in silicon integrated circuits," *Ieee Journal of Solid-State Circuits,* vol. 42, pp. 1678-1687, Aug 2007.

[9]   P. P. Pande, C. Grecu, A. Ivanov, and R. Saleh, "Design of a Switch for Network on Chip Applications," *Proc. Int'l Symp. Circuits and Systems (ISCAS)* vol. 5, pp. 217-220, May 2003.

[10]   A. W. Topol, D. C. La Tulipe, L. Shi, D. J. Frank, K. Bernstein, S. E. Steen, A. Kumar, G. U. Singco, A. M. Young, K. W. Guarini, and M. Ieong, "Three-dimensional integrated circuits," *Ibm Journal of Research and Development,* vol. 50, pp. 491-506, Jul-Sep 2006.

[11]   M. F. Chang et al., "RF Interconnects for Communications On-Chip," *Proceedings of International Symposium on Physical Design,* pp. 78-83, 13-16 April 2008.

[12]   M. J. Kobrinsky et al., "On-chip optical interconnects," *Intel Tech. J.,* vol. 8, pp. 129-142, May 2004.

[13]   W. M. J. Green, M. J. Rooks, L. Sekaric, and Y. A. Vlasov, "Ultra-compact, low RF

power, 10 gb/s silicon Mach-Zehnder modulator," *Optics Express,* vol. 15, pp. 17106-17113, Dec 10 2007.

[14]   D. Zhao and Y. Wang, "SD-MAC: Design and synthesis of a hardware-efficient collision-free QoS-aware MAC protocol for wireless Network-on-Chip," *Ieee Transactions on Computers,* vol. 57, pp. 1230-1245, Sep 2008.

[15]   G. W. Hanson, "On the applicability of the surface impedance integral equation for optical and near infrared copper dipole antennas," *Ieee Transactions on Antennas and Propagation,* vol. 54, pp. 3677-3685, Dec 2006.

[16]   G. Y. Slepyan, M. V. Shuba, S. A. Maksimenko, and A. Lakhtakia, "Theory of optical scattering by achiral carbon nanotubes and their potential as optical nanoantennas," *Physical Review B,* vol. 73, pp. -, May 2006.

[17]   P. J. Burke, S. D. Li, and Z. Yu, "Quantitative theory of nanowire and nanotube antenna performance," *Ieee Transactions on Nanotechnology,* vol. 5, pp. 314-334, Jul 2006.

[18]   G. W. Hanson, "Fundamental transmitting properties of carbon nanotube antennas," *Ieee Transactions on Antennas and Propagation,* vol. 53, pp. 3426-3435, Nov 2005.

[19]   Y. Huang, W. Y. Yin, and Q. H. Liu, "Performance prediction of carbon nanotube bundle dipole antennas," *Ieee Transactions on Nanotechnology,* vol. 7, pp. 331-337, May 2008.

[20]   R. I. Greenberg and H. C. Oh, "Universal wormhole routing," *Ieee Transactions on Parallel and Distributed Systems,* vol. 8, pp. 254-262, Mar 1997.

[21]   B. S. Feero and P. P. Pande, "Networks-on-Chip in a Three-Dimensional Environment: A Performance Evaluation," *IEEE TRANSACTIONS ON COMPUTERS,* vol. 58, pp. 32-45, January 2009.

[22]   F. Li et al., "Design and Management of 3D Chip Multiprocessors Using Network-in-Memory," *Proceedings of the 33rd International Symposium on Computer Architecture (ISCA),* pp. 130-141, 2006.

[23]   T. Theocharides et al., "Implementing LDPC Decoding on Network-On-Chip," *Proceedings of the International Conference on VLSI Design,* pp. 134-137, 2005.